Bound-constrained tomography for anisotropic and Q model building

Chaoguang Zhou, Samuel Brown and Zijian Liu, Petroleum Geo-Services*

Summary

Reflection tomography is an effective way to build anisotropic velocity and Q models for seismic imaging. However, reflection tomography suffers from a non-uniqueness problem, even when it only inverts for a single parameter, such as velocity (Stork, 1992). When anisotropy exists, surface seismic data alone cannot sufficiently determine the anisotropy parameters and there is ambiguity between them. Unconstrained reflection tomography may yield undesired or even non-physical models. To better constrain the tomographic inversion, additional information has to be incorporated into the system of equations. For example, Li et al. (2014) apply the results from stochastic rock physics modelling as an additional constraint to migration velocity analysis for anisotropic parameters. Zhou et al. (2014) incorporate well data into the ray-based tomographic equation system. In many cases, especially in frontier areas, little geologic or well information is available, complicating the process of model building. However, most likely the rough bounds of the model parameters in an area are known. Such bounds can be incorporated into the equation system as additional constraints. Vollebregt (2014) proposes a bound-constrained conjugate gradient algorithm for an optimization system constrained by positive solutions. In this paper, we generalize this algorithm to accommodate spatially variant lower and upper bounds for seismic model parameters and use these bounds to constrain reflection tomography.

Introduction

When the solution is limited to certain bounds, reflection tomography becomes a constrained optimization problem. For a global searching algorithm, for example, simulated annealing, the implementation of the bound constraints is straightforward. For gradient descent algorithms, there has been much research work and a variety of algorithms (Bertsekas, 1996) have been developed. Vollebregt (2014) proposes the Bound-Constrained Conjugate Gradient (BCCG) method that is a combination of the Conjugate Gradient method with the active set strategy. This method is appealing because it is simple and only requires minor changes to the conventional Conjugate Gradient algorithm. It is proposed to solve the linear system

$$\mathbf{A}\mathbf{x} = \mathbf{b}, \tag{1}$$

with the minimization objective function

$$\phi(\mathbf{x}) = \frac{1}{2}\mathbf{x}^T\mathbf{A}\mathbf{x} - \mathbf{b}^T\mathbf{x}, \; s.t. \quad \mathbf{x} \geq 0, \tag{2}$$

where T represents transpose.

Active set strategies solve the convex quadratic problems using a sequence of sub-problems in which the inequality constraints are partially ignored ("inactive constraints") and partially replaced by the simpler equalities ("active constraints"). In the BCCG method, the active set is changed aggressively by simply truncating variables that tend to cross their bounds. Namely, the projection is performed according to $\mathbf{x} = \max(0, \tilde{\mathbf{x}})$. Most bound-constrained Conjugate Gradient methods are too cautious in expanding the active set and are hampered by frequent restarting of the Conjugate Gradient iterations. The BCCG method, however, keeps the continuation of the Conjugate Gradient iterations and never restarts. This results in faster convergence and makes the BCCG method more appealing.

The joint reflection tomography for tilted transverse isotropy (TTI) model building can be expressed as the linear system (Zhou et al. 2010)

$$\mathbf{A}^T\mathbf{A}\mathbf{x} + \tau_S\mathbf{R}_S^T\mathbf{R}_S\mathbf{x}_S + \tau_\varepsilon\mathbf{R}_\varepsilon^T\mathbf{R}_\varepsilon\mathbf{x}_\varepsilon + \tau_\delta\mathbf{R}_\delta^T\mathbf{R}_\delta\mathbf{x}_\delta = \mathbf{A}^T\mathbf{b}, \tag{3}$$

where $\mathbf{x} = \mathbf{x}_s + \mathbf{x}_\varepsilon + \mathbf{x}_\delta$ and $\mathbf{x}_s, \mathbf{x}_\varepsilon$ and $\mathbf{x}_\delta$ are functions of model updates ΔS_{p0}, $\Delta\varepsilon$ and $\Delta\delta$. τ_s, τ_ε, and τ_δ are trade-off factors; $\mathbf{R}_S$, $\mathbf{R}_\varepsilon$ and $\mathbf{R}_\delta$ are the corresponding regularization operators.

The change caused by Q in the earth medium can be expressed as following (Brzostowski and McMechan, 1992):

$$-\frac{2}{\omega}\left[\frac{A}{A_0}\right] = \int Q^{-1}v^{-1}dl = \int Dv^{-1}dl, \tag{4}$$

where A and A_0 are the measured and reference spectra respectively; ω is the angle frequency; v is the seismic velocity; Q is the quality factor and $D=Q^{-1}$ is the dissipation factor. The left hand of equation (4) is referred to as t^*. The ray based tomography equation relates the residual t^* to the dissipation update:

$$\Delta t^* = \int \Delta D v^{-1} dl = \int \Delta D dt. \tag{5}$$

By adding a regularization term, equation (5) can be casted into a tomography system similar to equation (3):

$$\mathbf{A}^T\mathbf{A}\mathbf{x} + \tau_Q\mathbf{R}_Q^T\mathbf{R}_Q\mathbf{x} = \mathbf{A}^T\mathbf{b}. \tag{6}$$

The unknown vector **x** contains the dissipation factor updates; τ_Q is the trade-off factor and $\mathbf{R}_Q$ is the regularization operator. The linear systems (3) and (6) can be casted in the simpler form of equation (1) and the BCCG method can be generalized to solve this system subject to desired bound constraints.

Method

As previously mentioned, reflection tomography suffers from non-uniqueness. If we know the lower and upper limits of the velocity, epsilon and delta, we can add the following bound constraints to the joint reflection tomography to build a plausible anisotropic model:

$$\begin{aligned} &v_i \in [v^l, v^u], \\ &\varepsilon_i \in [\varepsilon^l, \varepsilon^u], \\ &\delta_i \in [\delta^l, \delta^u], \\ &i = 1,2,3....n. \end{aligned} \tag{6}$$

A similar constraint for Q tomography is

$$Q_i \in [Q^l, Q^u]. \tag{7}$$

These bound constraints are spatially variable because they are imposed on each model element individually. Also, each parameter has its own lower and upper bounds. The projection of the BCCG method has to be generalized to accommodate these bound constraints. First, we have to convert such constraints to x_i^l and x_i^u, the lower and upper bounds of the elements of the unknown vector **x**. The reason is that we do not directly solve for v, ε and δ or Q directly, as equations (30 and (6) indicate. Then, the projection is performed element-wise according to $x_i = \min(x_i^u, \max(x_i^l, x_i)), i = 1,2,3...$ One may notice that such a projection may result in undesirably rough models. To avoid this, a smoothness constraint can be imposed on the projection. The bound constraints (6) and (7) can also be expressed in terms of parameter updates instead of parameters themselves.

Following Vollebregt's recipe, the algorithm of the modified BCCG method consists of following steps.

0. Given an initial estimate $\tilde{\mathbf{x}}^0$ and spatially variable model parameter bounds. Convert the parameter bounds to the bounds of the elements of vector **x**. Project $\tilde{\mathbf{x}}^0$ element wise to construct the feasible initial model $\mathbf{x}^0$.

1. Start iteration k=1, 2, …, with given $\mathbf{x}^{k-1}$ and compute the gradient $\mathbf{g}^{k-1} = \mathbf{A}\mathbf{x}^{k-1} - \mathbf{b}$.

2. Construct the bound set B^k that contains the elements (bound variables) that are outside the lower and upper bounds, and the free set F^k that contains the elements (free variables) that are within the valid bounds.

3. Construct the search direction $\mathbf{p}^k$ that is zero in the components for the bound variables.
   a) Define the residual for the sub-problem corresponding to the free variables:
   $$r_i^{k-1} = \begin{cases} -g_i^{k-1}, i \in F^k \\ 0, i \in B^k \end{cases}.$$
   b) If k = 1, start with the steepest descent direction $\mathbf{p}^k = \mathbf{r}^{k-1}$.
   c) If $k > 1$, use conjugate gradients
   $$\beta^k = prod(\mathbf{r}^{k-1}, \mathbf{r}^{k-1} - \mathbf{r}^{k-2}) / prod(\mathbf{r}^{k-2}, \mathbf{r}^{k-2}),$$
   $$\mathbf{p}^k = \mathbf{r}^{k-1} + max(0, \beta^k)\mathbf{p}^{k-1}.$$

4. Compute the step size and iterate
   $$\mathbf{q} = \mathbf{A}\mathbf{p}^k,$$
   $$\alpha^k = prod(\mathbf{r}^{k-1}, \mathbf{p}^k) / prod(\mathbf{p}^k, \mathbf{p}^k),$$
   $$\tilde{\mathbf{x}}^k = \mathbf{x}^{k-1} + \alpha^k \mathbf{p}^k.$$

5. Project $\tilde{\mathbf{x}}^k$ element wise to get the feasible model $\mathbf{x}^k$.

6. Compute the gradient. If $\mathbf{x}^k \equiv \tilde{\mathbf{x}}^k$, this can be done with $\mathbf{g}^k = \mathbf{g}^{k-1} + \alpha^k \mathbf{q}^k$; Otherwise, the gradient is calculated with $\mathbf{g}^k = \mathbf{A}\mathbf{x}^k - \mathbf{b}$.

7. If convergence is reached, exit; Otherwise go back to step 1.

Field Examples

<u>VTI Model Building</u>

The bound constrained anisotropic model building is conducted on a narrow azimuth (NAZ) project in the North Sea. The earth medium is assumed to be VTI and the model building starts with a preliminary velocity field together with ε = 0 and δ=0. Significant residual moveouts are seen in the initial gathers (Fig. 2a). The events around the depth of 1600 m show much stronger far offset residuals, which indicates the existence of anisotropy. Joint reflection tomography (Zhou et al. 2011) is chosen for building the VTI model by simultaneously updating the vertical velocity and Thomsen parameters. Due to the poor δ resolution from surface seismic data (Zhou et al. 2011), an empirical δ/ε ratio of 2/3 is enforced in the tomographic equation system and therefore the three-parameter system becomes a two-parameter (velocity and ε) one. After four rounds of tomographic updating, the VTI model flattens the gathers (Fig. 3b). In general, the accumulated velocity updates (Fig. 1a) show increases above 2000 m and decreases below, corresponding to the event curving up in the upper portion of the initial gathers and curving down in the lower portion. The updated ε field (Fig. 2a) also shows similar pattern and the values range from -0.06 to 0.10. A large portion below 2500 m, where large negative velocity updates are seen, has negative ε values-the positive depth residuals in the lower portion of the initial gathers have been back projected into both negative velocity and ε updates. The negative ε values are not desired and it is caused by the leakage of velocity updates.

The same model building process with the same parameterization is repeated but with bound constraints $\Delta v \in [-1000.0,1000.0]$ and $\varepsilon \in [0,0.08]$. The resulting gathers (Fig. 3c) are comparable to the gathers (Fig. 3b) based on the VTI model built without the bound constraints. The accumulated velocity updates (Fig. 1b) show a similar pattern but with larger magnitudes than the cumulative velocity updates produced with the unconstrained tomography. In the lower part, the velocity is decreased by as much as 986 m/s compared to 585 m/s without the bound constraints. The updated ε field (Fig. 2b) shows overall smaller magnitudes (actual range [0, 0.07]) but with all positive values, as expected. The bound constraints stop the leakage of negative velocity updates into negative epsilon updates.

Q Estimation

The bound-constrained tomography is also used to build the Q model in another North Sea project. This area is characterized by gas anomalies with strong energy decay, which hamper the imaging of reflectors at the reservoir level. A detailed workflow can be found in Liu et al. (2016). When the tomography updates the Q model without the bound constraints, extreme values and non-physical (negative) values appear (Fig. 4a). When the bound constraint $Q \in [30,300]$ is imposed to the tomographic inversion, a plausible Q model (Fig. 4b) is produced. The depth slice at 1440 m overlain on the seismic stack shows a good match between the seismic image and the built Q model.

Conclusions

The process of building anisotropic velocity and Q models suffers from non-uniqueness, and unconstrained tomography may yield undesired or even non-physical models. When the limits of the model parameter values are known, they can be imposed as additional constraints in the tomography system of equations to help produce geologically plausible anisotropic velocity or Q models. As demonstrated in the examples, the generalized Bound-Constrained Conjugate Gradient method is an effective method to solve such bound constrained tomographic systems.

Acknowledgements

The authors thank colleague Dennis van der Burg for providing the pre-processed seismic data and the initial velocity model. The authors also thank PGS for the permission to publish this abstract.

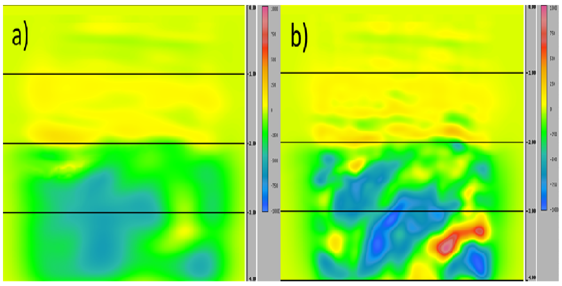

Figure 1: The accumulated velocity updates: a) without the bound constraints; b) with the bound constraints.

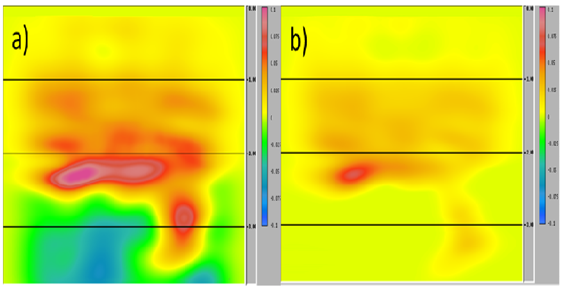

Figure 2: The updated ε fields: a) without the bound constraints; b) with the bound constraints.

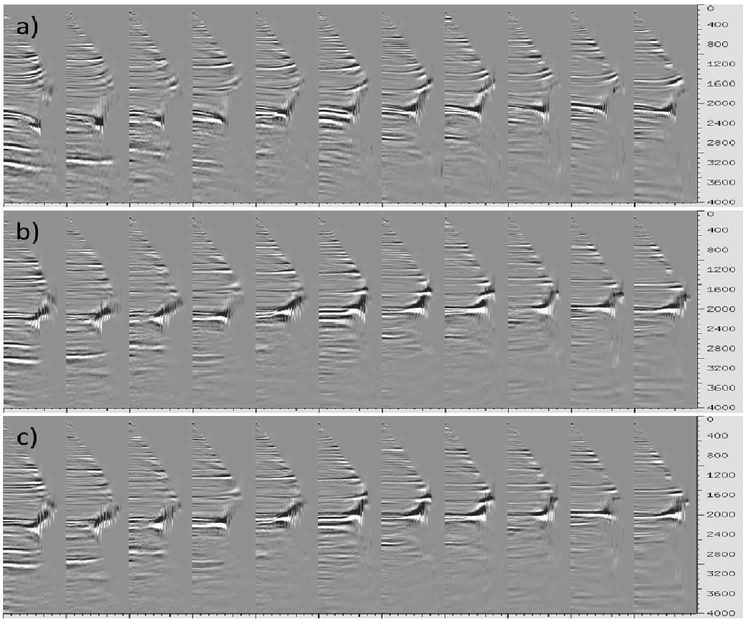

Figure 3: The CIG gathers: a) the starting gathers; b) the final gathers based on the model built without the bound constraints; c) the final gathers based on the model built with the bound constraints.

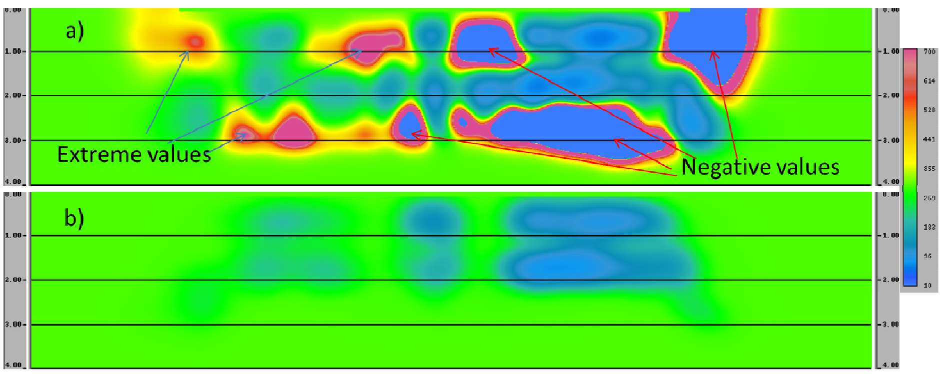

Figure 4: Tomographically updated Q models: a) without the bound constraint (values are clipped) and b) with the bound constraint.

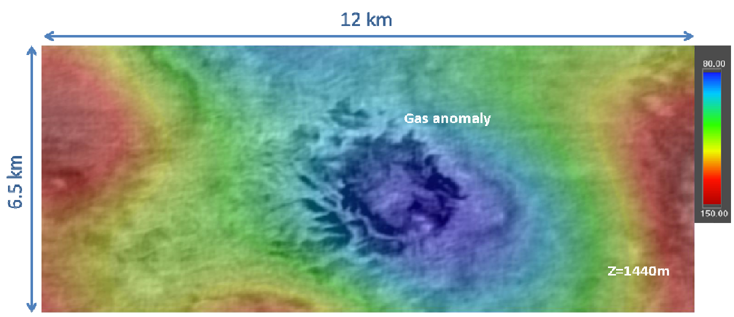

Figure 5: The depth slice of the updated Q model overlaid on the seismic image.

EDITED REFERENCES

Note: This reference list is a copyedited version of the reference list submitted by the author. Reference lists for the 2016 SEG Technical Program Expanded Abstracts have been copyedited so that references provided with the online metadata for each paper will achieve a high degree of linking to cited sources that appear on the Web.

REFERENCES

Bertsekas, D. P., 1996, Constrained optimization and Lagrange multiplier methods: Athena Scientific.

Li, Y., D. Nichols, and G. Mavko, 2014, Stochastic rock physics modeling for seismic anisotropy: 84th Annual International Meeting, SEG, Expanded Abstracts, 2899–2904, http://dx.doi.org/10.1190/segam2014-0299.1.

Liu, Z., S. Brown, A. Valenciano, and N. Chemingui, Simultaneous Q and velocity model building-incorporating attenuation to enhance model resolution: 78th Annual International Conference and Exhibition, EAGE, Extended Abstracts, 29643.

Stork, C., 1992, Reflection tomography in the postmigrated domain: Geophysics, **57**, 680–692, http://dx.doi.org/10.1190/1.1443282.

Vollebregt, E. A. H., 2014, The bound-constrained conjugate gradient method for non-negative matrices: Journal of Optimization Theory and Applications, **162**, 931–953, http://dx.doi.org/10.1007/s10957-013-0499-x.

Zhou, C., J. Jiao, S. Lin, J. Sherwood, and S. Brandsberg-Dahl, 2011, Multi-parameter joint tomography for TTI model building: Geophysics, **76**, no. 5, WB183–WB190, http://dx.doi.org/10.1190/geo2010-0395.1.

Zhou, C., Z. Liu, N. D. Whitmore, and S. Brown, 2014, Anisotropic model building with well control: 84th Annual International Meeting, SEG, Expanded Abstracts, 4675–4679, http://dx.doi.org/10.1190/segam2014-1345.1.